Scientific paper

Kinetic Studies, Antioxidant Activities, Enzyme Inhibition Properties and Molecular Docking of 1,3-Dihydro-1,3-Dioxoisoindole Derivatives

Hasan Yakan,[1,*] Seyhan Ozturk,[2] Elvan Uyar Tolgay,[2] Semiha Yenigun,[2] Sarmad Marah,[2] Tugrul Doruk,[3] Tevfik Ozen[2,*] and Halil Kutuk[2]

[1] *Ondokuz Mayis University, Faculty of Education, Department of Chemistry Education, 55139, Atakum-Samsun, Turkey.*

[2] *Ondokuz Mayis University, Faculty of Sciences, Department of Chemistry, 55139, Atakum-Samsun, Turkey.*

[3] *Ondokuz Mayis University, Faculty of Sciences, Department of Molecular Biology and Genetics, 55139, Atakum-Samsun, Turkey.*

* *Corresponding author: E-mail: E-mail:hasany@omu.edu.tr; tevfkoz@omu.edu.tr*

Received: 11-18-2022

Abstract

The acid catalyzed hydrolysis of the *N*-(*p*-substitutedphenyl) phthalimides in three different acids was investigated at 50.0 ± 0.1 °C. Two different antioxidant activity tests as $DPPH^{\bullet}$ and $ABTS^{\bullet+}$ scavenging activities, and three various enzyme inhibition activity tests as urease, acetylcholinesterase (AChE), and butyrylcholinesterase (BChE) inhibition activities, were applied. Compound **3c** (2.03 μg/mL) has higher antioxidant activity than other compounds and standards according to DPPH test. In AChE assay, compounds **3a** and **3b** (13.13 and 9.59 μg/mL) has higher enzyme inhibition activity than the standard Galantamine (14.37 μg/mL). In BChE and urease tests, all compounds (6.84-13.60 and 10.49-17.73 μg/mL) have higher enzyme inhibition activity than the standard Galantamine (49.40 μg/mL) and thiourea (26.19 μg/mL), respectively. The molecule interaction for each of the three compounds with the active sites of AChE, BChE, and urease enzymes was examined via molecular docking simulations.

Keywords: Arylphthalimides; Kinetic Studies; Acid-Catalyzed Hydrolysis; Antioxidant Activity; Enzyme Inhibitor; Molecular Docking.

1. Introduction

Phthalimides (1,3-dihydro-1,3-dioxoisoindoles) are a significant class of drugs showing antimicrobial,[1] antibacterial,[2] antituberculosis,[3] cytotoxicity,[4] anticancer,[5] analgesic,[6] acetylcholinesterase inhibitors,[7] an inhibitor of nitric oxide synthase to human neuronal,[8] and antiproliferative.[9] These compound's derivatives showed various biological activities, were substantiated as an exciting pharmacophore and could interact with the peripheral anionic site of the enzymes. Some phthalimides synthesize as multi-function compounds and are determined to be a stabled multi-target active molecule that showed strong and stable activities against urease and cholinesterase inhibitors.[10]

They have recently attracted a noticeable amount of attention due to their interesting anti-inflammatory,[11] and anti-angiogenic specialties and their possible use in treating AIDS reasoned by HIV.[12] Because of its pharmaceutical, biological, and industrial importance, the synthesis of *N*-arylphthalimides has attracted considerable interest in the literature.[13] *N*-Arylphthalimides have been commonly prepared with a phthalic acid anhydride and primary amines. This is the most known method in the literature.[14]

Antioxidants are the reducing agents that have been used to balance many free radicals. Free radicals are groups of atoms or atoms with a single number of electrons. They can be composed that oxygen molecules interacting with specific molecules in drugs, atmospheric pollutants, and mitochondrial respiratory chain reactions. Free radicals are dangerous to persons and harm all fundamental components of cells, with the inclusion of proteins, cell membranes, and DNA, and reason for various pathological statuses such as myocardial infarction, diabetes mellitus, atherosclerosis, asthma, arthritis, inflammation, neurodegenerative, carcinogenesis, and anemia diseases.[15] Non-enzymatic and enzymatic antioxidants may avoid this oxidative damage in the human body. Still, it

may disrupt these protective mechanisms and the various pathological processes and, therefore, the reason for damage.[16]

Acetylcholinesterase (AChE) is cared for with the growth of cells and aids the development of regeneration of nerves and neurons.[17] AChE is a significant member of the nervous system; therefore, adverse effects on AChE activity can induce neurotoxicity.[18] Butyrylcholinesterase (BChE) is connected to physical factors such as the hydrolysis of noncholine and choline esters. Consequently, it has an essential role in neurotransmission and anesthesia.[19] A significant rise in acetylcholinesterase activity is spied in Alzheimer's disease (AD) early phase, yet, the butyrylcholinesterase activity progressively advances in Alzheimer's late grades. Therefore, both BChE and AChE are pretty medicinal aims to improve the cholinergic explicit and idea the AD.[20] Urease enzyme inhibitors can enter into a vital to against the negative effect of urease in living organisms. These inhibitors are efficient against a few crucial infections induced by the secretion of urease by *Helicobacter pylori*.[21] This bacteria releases urease, and the excretion of ammonia defends it from the acidic medium of the stomach.[22]

In recent years, molecular docking tectechniquesere were performed upon massive enzyme numbers, including urease and cholinesterase. This study is used to understand and provide important information about the powerful binding of the inhibitor and enzymes through a set unlike protein-ligand interactions.[23] It is also repeatedly used to anticipate the binding orientation of ligands to the target protein/s and assess the candidate inhibitor's binding affinity, activity, and stability.[24]

Acid-catalysed reactions as general and specific acid catalysis come off the two distinct ways.[25] Generally, acidic kinds catalyse the reaction according to their own characteristics. The substrate protonation becomes the rate-determining step, and the conjugate acid of the substrate reaction products in a quick step.[25] The only source of protonation is H_3O^+ in specific reactions that are acid-catalysed, which can occur in two distinct processes. A unimolecular mechanism A-1, a protonated substrate formed in the rate-limiting step and afterward transforms quickly into products (Eq.1 in Scheme 1). If the nucleophile attacks the protonated substrate (Nu; e.g., always water) in the rate-limiting step, a bimolecular mechanism A-2 is described (Eq.2 in Scheme 1).[25] Since the reaction mechanism is firmly specified under low acidity and high acidity conditions, a series of standards that meet the kinetic data, such as the order of acid catalytic efficiency,[26] shapes of profiles,[27] excess acidity treatment,[28] thermodynamic data,[29] and affection of substituent[30] are available.

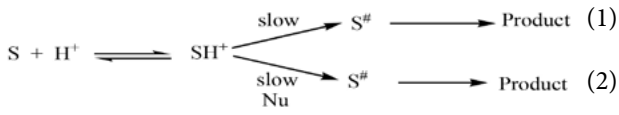

Scheme 1. Specific acid-catalysed reactions. (1) Unimolecular reaction A-1, (2) Bimolecular reaction A-2

A bimolecular mechanism at low acidity is indicated by substituent effect, entropy effects and excess acidity method, with analysis of the data by the Cox–Yates.[31] A unimolecular mechanism is observed at higher acidities. A unimolecular mechanism has $\Delta S^{\neq}$ of about 0 to -41.7 JK^{-1} mol^{-1}, while the reaction with a bimolecular mechanism has $\Delta S^{\neq}$ of -62.8 to -125.6 JK^{-1} mol^{-1} in the acid-catalyzed hydrolysis of compounds proceeding [29]. The kinetic studies of amidosulfites,[32] *N*-(4-substitutedarylsulfonyl) phthalimides,[33] (4-methoxybenzoyl)-4-tolueniminosulfonate,[34] and *N*-(4-substitutedarylthio) phthalimides[35] have been reported in the literature. There are no kinetic studies, and biological evaluations have been conducted on the *N*-(4-substitutedaryl) phthalimides. This work, it was aimed to obtain more information about kinetic studies and acidic hydrolysis activity of a series of *N*-(4-substitutedaryl) phthalimides **3a-c.** Moreover, antioxidant activities of the compounds were determined with two specific tests as DPPH· and $ABTS^{\cdot+}$ scavenging methods and were investigated three various enzyme inhibition activities as urease, acetylcholinesterase, and butyrylcholinesterase. Molecular docking simulations was used for the molecule interaction for each of the three compounds with the active sites of acetylcholinesterase, butyrylcholinesterase, and urease enzymes.

2. Experimental

2. 1. General Remarks

Sigma, Riedel-de Haën, and Merck, what provide the all reagents used. The ^1H and ^{13}C NMR spectra were determined on a Bruker Avance 300 MHz Spectrometer (Germany) at 300 MHz and 75 MHz, respectively, in $CDCl_3$ using tetramethylsilane as the internal calibration standard. IR spectra were saved with a Vertex 80v FT-IR (Germany). Melting point measurements were made by Electrothermal 9100 Melting Point Apparatus (China). Kinetic measurements of all compounds were obtained with a GBC Cintra 20 model Ultraviolet-Visible (UV-VIS) Spectrophotometer (Australia).

2. 2. Synthesis

A mixture of phthalic anhydride (5 mmol) and aniline (5 mmol) was dissolved in acetic acid (25 mL). Also, sulphamic acid (10 mol%) was added as a catalyst. The reaction mixture was refluxed at 110 °C for 10 minutes. After that, the reaction mixture was poured into water. The solid was collected by filtration under vacuum, washed with ethyl acetate, and recrystallized in ethanol to give **3a-c** as white crystals in Scheme 2. The products were prepared with minor modifications according to a reported procedure [36].

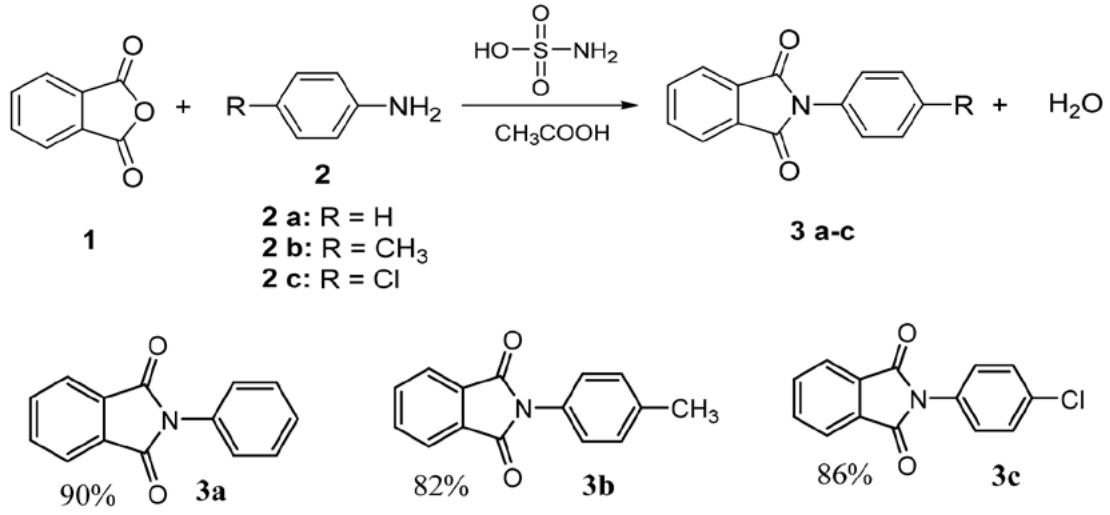

Scheme 2. Synthesis of 1,3-dihydro-1,3-dioxoisoindoles (**3a-c**)

*N-(Phenyl)phthalimide (**3a**):* White solid (0.98 g, 90%); m.p. 207 °C; Lit.[37] m.p. 206 °C; IR (KBr) (ν_{max}, cm^{-1}): 3088, (Ar. CH), 1745–1708 (C=O), 1160 (C-N); ^{1}H NMR (300 MHz, $CDCl_3$) (δ, ppm): 8.01–7.78 (4H, m, Arom.), 7.56–7.40 (5H, m, Arom.); ^{13}C NMR (75 MHz, $CDCl_3$) (δ, ppm): 167.3 (C=O), 134.3, 133.2, 131.6, 129.7, 127.4, 124.6, 121.8 (Arom.C); found C, 75.23; H, 4.14; N, 6.27; calc. for $C_{14}H_9NO_2$ C, 75.33; H, 4.06; N, 6.27%.

*N-(4-Methylphenyl)phthalimide (**3b**):* White solid (0.97 g, 82%); m.p. 202–203 °C; Lit.[37] m.p. 204 °C; IR (KBr) (ν_{max}, cm^{-1}): 3064, (Ar. CH), 2958 (-CH_3), 1734–1713 (C=O), 1153 (C-N); ^{1}H NMR (300 MHz, $CDCl_3$) (δ, ppm): 7.99–7.94 (4H, m, Arom.), 7.84–7.79 (4H, m, Arom.), 2.38 (3H, s, -CH_3); ^{13}C NMR (75 MHz, $CDCl_3$) (δ, ppm): 166.4 (C=O), 136.8, 135.1, 133.6, 131.3, 129.7, 127.9, 122.8 (Arom. C), 21.3 (-CH_3); found C, 76.31; H, 4.68; N, 6.00; calc. for $C_{15}H_{11}NO_2$ C, 75.94; H, 4.67; N, 5.90%.

*N-(4-Chlorophenyl)phthalimide (**3c**):* White solid (1.10 g, 86%); m.p.196 °C Lit.[38] m.p. 194–195 °C; IR (KBr) (ν_{max}, cm^{-1}): 3043, (Ar. CH), 1731–1718 (C=O), 1159 (C-N), 873 (C-Cl); ^{1}H NMR (300 MHz, $CDCl_3$) (δ, ppm): 8.01–7.79 (4H, m, Arom.), 7.55–7.41 (4H, m, Arom.); ^{13}C NMR (75 MHz, $CDCl_3$) (δ, ppm): 168.4 (C=O), 135.6, 133.4, 132.8, 131.3, 129.7, 128.9, 127.7, 123.0. (Arom.C); found C, 64.51; H, 3.11; N, 5.42; calc. for $C_{14}H_8ClNO_2$ C, 65.26; H, 3.13; N, 5.44%.

2. 3. Kinetic Procedure

The hydrolysis rate of the substrate **3a-c** were measured at a wavelength of 231–241 nm at 50.0 ± 0.1 °C. The kinetic run was started for all compounds by injecting 20 μL of 1.0×10^{-2} M substrate stock solution in acetonitrile into the 3.0 mL acid solution equilibrated at 50.0 ± 0.1 °C in a quartz cuvette. The course of reactions was monitored over (at least) up to three half-lives and the absorbance values at infinity were acquired after ten half lives in all cases. Good first-order behaviour was observed with clean isosbestic points. The values of pseudo first-order rate constants (k_1) were calculated from the plots of $ln(A\text{-}A\infty)$ against time using the least squares procedure, where A is the absorbance at time t and $A\infty$ is the absorbance at infinity.[39] All kinetic runs were duplicated and the average deviation from the mean was less than < 3%. Deionized water, HPLC grade acetonitrile, and analytical grade concentrated acid were used to prepare all acid reaction solutions, making appropriate allowance for the water content of the acid.

2. 4. Product Analysis

Analysis of the product performed resulting from acid-catalyzed hydrolysis of *N*-(4-chlorophenyl) phthalimide was determined using the melting point comparison and spectroscopic (IR, NMR) methods. The products were thought of as phthalic acid and 4-chloroaniline. To determine products at the end of the reaction, we studied the same condition of the kinetic procedure. For this, 0.4 g of *N*-(4-chlorophenyl) phthalimide was allowed to react with 15 mL, 7.00 M HCl at 50.0 ± 0.1 °C for 6 hours. After the completion of the reaction, the solid white product was filtered and purified. The solid was crystallized from ethyl alcohol to give the expected products (phthalic acid). The melting point of the crystalline solid was found at 207–208 °C. The melting point of phthalic acid is 210–211 °C.[40] IR (KBr) (ν_{max}, cm^{-1}): 3093–2686 (–COOH, including Arom.

CH and Aliph.CH), 1721–1695 (C=O), 1283 (C-O). ^{1}H NMR (400 MHz, $CDCl_3$) (δ, ppm): 13.1–12.7 (2H, s, COOH), 8.02–7.75 (4H, m, Ar). ^{13}C NMR (75 MHz, $CDCl_3$) (δ, ppm): 169.1 (C=O), 132.5, 131.2, 129.3 (Ar C). Finally, it was determined by IR, NMR, and melting point comparisons that these values are consistent with data in the literature.

2. 5. Antioxidant Evaluation

Free Radical Scavenging Activity (DPPH˙)

DPPH˙ activity of the samples was determined using the DPPH• (1,1-diphenyl-2-picryl-hydrazil) method [41]. 150 µL of distinct concentrations of samples or standards (TBHQ, α-tocopherol, and BHA), and 50 µL of 0.1 mM DPPH• have homogeneously mixed in a 96-well plate. The samples have waited in the dark at room temperature for 30 min. The absorbance values of each mixture were measured at 517 nm using the BIOTEK (Epoch2) microplate reader and determined the results by calculating the IC_{50} (µg/mL) values. The activity for DPPH˙ scavenging was calculated by the following equation[41]:

The percentage activity,

$$\% = [(A_{control,\ 517\ nm} - A_{sample,\ 517\ nm})/A_{blank,\ 517\ nm}] \times 100.$$

ABTS˙⁺ Radical Scavenging Activity

ABTS˙⁺ radical scavenging activity of the samples was performed using the ABTS-K_2SO_8 method[42]. 2.45 mM K_2SO_8 and 7 mM ABTS (1:2) were mixed and incubated for 12–16 hours at room temperature in the dark. The mixture was diluted with ethanol so that the absorbance value was 0.700 ± 0.020. 20 µL of different concentrations of samples or standards (BHA, TBHQ, and α-tocopherol), and 180 µL of ABTS•⁺ solution were mixed homogeneously in a 96-well plate. The absorbance value of each mixture was measured after 6 min at 734 nm using the BIOTEK (Epoch2) microplate reader, and the results were determined by calculating the IC_{50} (µg/mL) values.

ABTS˙⁺ scavenging activity (%) = [1− (absorbance of sample/absorbance of blank)] × 100

2. 6. Enzyme Inhibition Activity

Urease Inhibition Activity

The urease inhibition activity of the samples was determined using the indophenol method[43]. In a 96-well plate, 10 µL of samples or thiourea at different concentrations, 25 µL of 1 U urease (in 100 mM pH 8.2 sodium-potassium buffer), and 50 µL of 17 mM urea were mixed homogeneously. The samples were incubated for 15 minutes at 30°C. Mixture is homogeneously mixed with 45 µL of phenol reagent (0.1% (w/v) sodium nitroprusside and 8% (w/v) phenol) and 70 µL of alkaline reagent (4.7% (v/v) NaOCl and 2.5% (w/v) NaOH) solutions mixed. The samples were kept at 30 °C for 50 min. The absorbance values of each mixture were measured at 630 nm using a BIOTEK (Epoch2) microplate reader, and presentedthe IC_{50} (µg/mL) values of the results by calculated.

AChE and BChE Inhibition Activity

AChE and BChE inhibition activities of the samples were determined by using the Ellman method[44]. 20 µL of samples or galantamine at different concentrations in a 96-well plate, 20 µL of 0.03 U AChE or BChE (in 100 mM pH 8.0 sodium-potassium buffer), 20 µL of 3.3 mM DTNB, and 140 µL of 100 mM pH 8.0 sodium-potassium buffer mixed homogeneously. The samples have incubated for 15 min at room temperature. The mixture has combined homogeneously by adding 10 µL of 1 mM acetylcholine iodide or butyrylcholine chloride. The absorbance values of each mix were measured at 412 nm using a BIOTEK (Epoch2) microplate reader and found the results by calculating the IC_{50} (µg/mL) values.

2. 7. Molecules Preparation and Docking Protocol

All synthesized compounds were drawn in ChemDraw Ultra 18.0 and then by their geometry optimization (energy-minimized) with Chem3D 18.0. The optimized structures were saved in Mol2 format. The rotation ability for rotatable bonds in the flexible residues was detected automatically by the AutoDock Tools version 1.5.4 program. Then, synthesized compounds **3a–c** were optimized using AutoDock Tools software before the docking procedure.

All of the used protein 3D structure was retrieved from Protein Data Bank (RCSB PDB: an information portal to biological macromolecular structures), all enzymes' structure were selected due to their high resolution of 2 angstroms (Å) or less, and the program generated satisfactory solutions with this range of resolution[45]. The crystal structure of Jack bean urease with PDB-ID 4GY7 at 1.49 Å resolution. On the other hand, the crystal structure of the human enzyme had been selected for acetylcholinesterase and butyrylcholinesterase with PDB-ID 4M0E and 1P0I, respectively; both enzyme structures had resolution at 2 Å. We also used the AutoDock Tools software for the enzyme macromolecules preparation. After removing non-standard residues and water molecules from enzymes, polar hydrogens were added to the macromolecule to reach the protonation state; then, enzymes coordinate were adjusted using the same program.

AutoDock vina tool has been used to predict the most appropriate binding site of the synthesized compounds **3a–c** within target enzymes[46]. Those results, the solution that reached the minimum estimated Gibbs binding energy, was saved as the top-scoring mode. The graphical representation of the docked poses was rendered in PyMOL version 2.5 software for the 3D. To obtain the 2D

structure of the interactions between compounds and target enzymes and the Ligplot+ 2.2.4 program wasused[47].

2. 8. Statistical Analysis

The results of triplicate analysis obtained from *in vitro* biological activity studies were expressed as ± standard deviation values for each parameter. All data were analysed in the IBM Statistical Package for Social Studies (SPSS) 20.0 program. One-way ANOVA has been used because the means of more than two independent groups between the analysis averages and the variances with normal distribution in the data were homogeneous. Tukey HSD[a,b] was used for multiple comparisons with the data obtained. The statistical significance level of the values compared with the activity analysis result group and the significance level was expressed with $p < 0.05$ deals and considered statistically significant.

3. Results and Discussion

3. 1. Kinetic Studies

First-order rate coefficients, k_1, in the hydrolysis of *N*-(phenyl) phthalimide **3a** in the studied acid solutions are given in Figure 1. Increasing the concentration of acids in the worked range raised the hydrolysis rates continuously in all cases. There is no sign of maximum rate even at pretty high acidity.

The order of catalytic effectiveness of the acids obtained for the hydrolysis of **3a** was HCl ≅ H_2SO_4 > $HClO_4$ or H_2SO_4 ≅ HCl > $HClO_4$ in the whole range of acidity. Bunton and his co-workers[48] put forward that such an order is characteristic of a bimolecular mechanism, for the transition states of positive character are preferably stabilized by anions of high charge density such as Cl^-, while the opposite is usually the case for a unimolecular mechanism[26a,48].

The kinetic data obtained using the Cox and Yates Excess Acidity method [31] are shown in Table 1. Eq.3 is used in a simplified form of the equations for unprotonated substrates.

$$\log k_1 - \log C_{H^+} - [\log Cs / (Cs + C_{SH^+})] = m^* m^{\neq} X + r \log a_{Nu} + \log (k_0 / K_{SH^+}) \quad (3)$$

In equation (3), k_1 is the pseudo-first-order rate constant in aqueous acid concentration C_{H^+} and of Excess Acidity X and $m^* m^{\neq}$ are the slope parameter, where $m^{\neq}$ is characteristic of the type of reaction (for an A-1 process $m^{\neq} > 1$; an A-2 processes $m^{\neq} \cong 1$) and m^* is obtained from protonation studies $r \log a_{Nu}$ for the bimolecular reaction

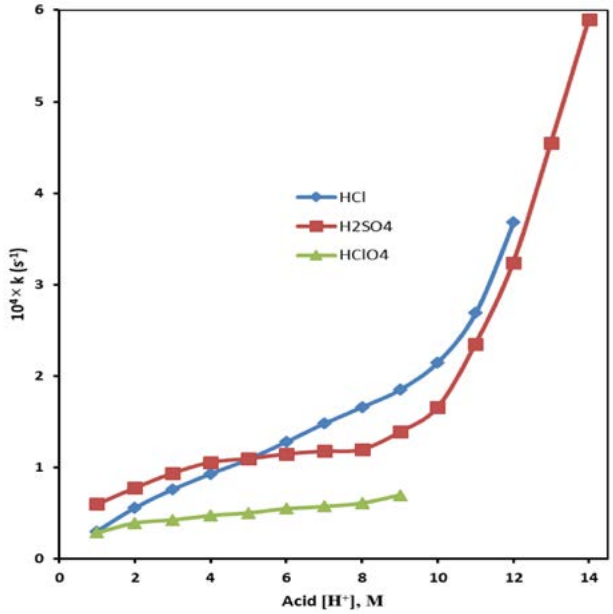

Figure 1. Plots of k_1 plots of different aqueous acid solutions for acid-catalyzed hydrolysis of **3a** at 50.0 ± 0.1 °C (●,HCl; ■,H_2SO_4; ▲, $HClO_4$)

Table 1. $10^4 k_1$ (s^{-1}) Values for the hydrolysis of the synthesized compounds at 50.0 ± 0.1°C

[H⁺]/M	3a			3b			3c		
	H_2SO_4	$HClO_4$	HCl	H_2SO_4	$HClO_4$	HCl	H_2SO_4	$HClO_4$	HCl
1	0.60	0.38	0.30	0.001	0.001	0.01	102	18.3	55.0
2	0.78	0.40	0.56	0.002	0.002	0.02	156	34.6	96.2
3	0.94	0.43	0.76	0.004	0.003	0.03	227	42.6	154.1
4	1.06	0.48	0.97	0.006	0.004	0.04	376	57.4	224.0
5	1.10	0.50	1.09	0.015	0.008	0.07	465	38.2	134.6
6	1.15	0.55	1.28	0.035	0.025	0.13	345	21.3	71.3
7	1.18	0.58	1.48	0.300	0.055	0.18	212	13.3	42.8
8	1.20	0.61	1.67	0.420	0.090	0.22	102	3.44	18.9
9	1.39	0.70	1.85	0.650	0.150	0.35	67	3.30	12.6
10	1.66	–	2.05	0.800	–	0.48	43	–	8.3
11	2.35	–	2.37	0.940	–	0.57	32	–	5.7
12	3.24	–	3.01	1.320	–	0.69	21	–	3.9
13	4.55	–	–	1.680	–	–	11.4	–	–
14	5.90	–	–	1.860	–	–	7.2	–	–

represents the activity of the nucleophile, where r is the number of water molecules involved in the formation of the transition state [31].

Because of low basicity of the synthesized compounds, the protonation correction term [log Cs / (Cs + C_{SH^+})] is negligible. X values were used for aqueous solution of the acid[31b,49].

The graph of log k_1 – logC_{H^+} versus X for the hydrolysis of **3a** in HCl solution is shown in Figure 2. Similar plots were observed for **3b** and **3c** in HCl solution. In beginning, all such plots of arylphthalimide in the low acidity region showed downward curvature, which is a typical feature of A-2 reactions involving water [27].

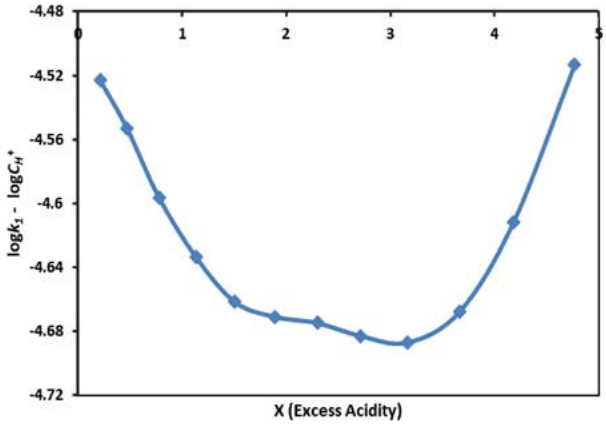

Figure 2. Plots of excess acidity versus logk_1-logC_{H^+} for the hydrochloric acid-catalysed hydrolysis of **3a** at 50.0 ± 0.1°C

Show in Figure 2, in the 1.00–8.00 M region with increasing acid concentration, the plot shows that the rate of reaction was diminished, and there was no catalytic impact of the acids. Water activity decreases with acid concentration increases and the reaction rate decreases due to the decrease in water activity. After 8.00 M with acid concentration increases, the rate of hydrolysis increases, and there was consist of a catalytic effect of the acids. A curve was formed at 8.00–12.00 M acidity region. A straight line was seen in the acidity region (8.00–12.00 M); values of 2loga_{H2O} can be obtained from the left-hand side of Eq. (3), and the result was plotted against X. Straight-line correlation (Figure 3 and Table 1 where r = 2) was determined for aryl phthalimides. According to this evidence, two moles of water was detected in the reaction rate-determining step of the A–2 mechanism.

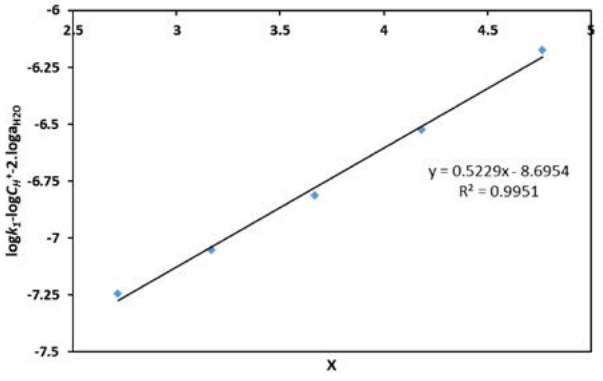

Figure 3. Plots of excess acidity versus log k_1-logC_{H^+}–2.loga_{H2O} for the 8.00–12.00 M hydrochloric acid-catalyzed hydrolysis of **3a** at 50.0 ± 0.1°C

The relationship between temperature and rate constants was analyzed by a spreadsheet program (Eyring equation) using at least a square program. The values at different temperatures and Arrhenius parameters (Eq. 4) are shown in Tables 2 and 3, respectively.

$$k = \frac{k_B.T}{h}.\exp\left(-\Delta H^{\neq} / RT\right).\left(\Delta S^{\neq} / R\right) \quad (4)$$

Acid catalyzed hydrolysis of amides and esters [29] proceeding by an A-1 mechanism have $\Delta S^{\neq}$ of about 0 to –41.8 Jmol^{-1}K^{-1}, while those proceeding by an A-2 mechanism have $\Delta S^{\neq}$ of –62.8 to –125.5 Jmol^{-1}K^{-1}. For the hydrolysis of **3a** in 4.00 M and 8.00 M hydrochloric acid, the values of $\Delta S^{\neq}$ are –89.57, –71.69 Jmol^{-1}K^{-1}, respectively. Moreover, the values for the hydrolysis of **3b** and **3c** change similarly, as expected. Also, hydrolysis of **3a** in 4.00 M and 8.00 M sulfuric and perchloric acid, the values of $\Delta S^{\neq}$ are –93.84, –71.69, –101.63, and –99.51 Jmol^{-1}K^{-1}, respectively. In an A-2 mechanism, negative values of $\Delta S^{\neq}$ indicate that the water molecule behaves like a nucleophile. In the acidity range studied, electron-withdrawing substituents cause the highest rate of hydrolysis (**3c>3b**), and the substituent effects are well correlated by a satisfactory Hammett $\rho\sigma$ plot [at 8.00 M HCl, ρ = 4.847 (corr. 0.9987)] as shown in Figure 4. Noticeably at these acidities, the electron-withdrawing group enhances the nitrogen atom's positive charge. Therefore, the nucleophilicity of the water molecules becomes more effective on account of the positively charged nitrogen atom in the reaction rate-determining transition state for the A-2 mechanism.

However, [e.g. 4.00 M H_2SO_4, ρ = 13.11 (corr. 0.9998)] as shown in Figure 5, **3c** hydrolysis was more rapid than **3b.** It is predominantly consistent with the bimolecular mechanism that substituent effects on the protonation and slow step operate in opposite directions. Similar behaviours have been observed for the hydrolysis of arylsulfonyl phthalimides [33] and substitutedarylthio phthalimides [35] an A-2 mechanism at lower acidities. 2.00 M $HClO_4$, ρ = 0.848 (corr. 0.9997) for *N*-(4-bromophenylsulfonyl) phthalimides hydrolysis was more rapid than *N*-(4-methylphenylsulfonyl) phthalimides, and consistent with a predominantly an A-2 mechanism. Likewise, 1.00 M $HClO_4$, ρ = 0.803 (corr. 0.996) for *N*-(4-chlorophenylthio) phthalimides hydrolysis was more rapid than *N*-(4-methylphenylthio) phthalimides. There is no direct evidence concerning the site of protonation of *N*-(4-substitutedaryl) phthalimides; however, *N*-(4-substitutedarylsulfonyl) phthalimides[33], *N*-(4-substitutedarylthio) phthalimides[35], and *N,N′*-diarylsulfamides[39] occurs pref-

erentially at the nitrogen atom. In addition, $m^*m^{\neq}$ are the combined slope parameters, where m^* gives information about the protonation site (for nitrogen m^*: 0.65–1.40; oxygen m^*: 0.13–0.60; sulfur m^*: 1.25–1.80; carbon m^*: 1.4–2.02)[50]. For compound **3a**, $m^*m^{\neq}$ slope parameters in various acids HCl (8.00–12.00 M), H_2SO_4 (8.00–12.00 M) and $HClO_4$ (6.00–9.00 M) are 0.52, 1.29, and 0.76, respectively (see at S11 and S13 in supplementary information). A value of m^*= 1.025 is assume for protonation on nitrogen. It was found that $m^{\neq}$ is 0.51, 1.26, and 0.74 for HCl, H_2SO_4, and $HClO_4$, respectively. According to the observations, the nitrogen atom is most likely the protonation site of all the compounds.

Based on the overall arguments available, we suggested the acid-catalyzed hydrolysis mechanism of the compounds improves with an A-2 mechanism in the whole range of acidity as given in Scheme 3. In the first, occur quick pre-equilibrium protonation of the arylphthalimide. It is assumed that protonation occurs on a nitrogen atom, and two water molecules attack the car-

Table 2. $10^4 k_1$ (s^{-1}) Values for the hydrolysis of the **3a-c** at varied temperatures (°C)

Acid (M)	Compounds	30.0	35.0	40.0	45.0	50.0	55.0	60.0
4.00 M HCl	**3a**			0.39	0.68	0.93	1.53	2.29
8.00 M HCl	**3a**			0.75	1.24	1.67	2.93	4.86
4.00 M H_2SO_4	**3a**			0.44	0.70	1.06	1.54	2.51
8.00 M H_2SO_4	**3a**			0.45	0.81	1.20	1.87	3.01
6.00 M $HClO_4$	**3a**			0.20	0.35	0.55	0.74	1.13
8.00 M $HClO_4$	**3a**			0.25	0.38	0.61	0.87	1.41
4.00 M HCl	**3b**			0.02	0.03	0.04	0.08	0.12
4.00 M HCl	**3c**	54	74	102	158	224		

Table 3. Values of $\Delta H^{\neq}$ and $\Delta S^{\neq}$ for the hydrolysis of the synthesized compounds

Compounds	Acid	[H^+] / M	$\Delta H^{\neq}$ (kJ/mol)	$\Delta S^{\neq}$ (J/molK)	Temperature Range (°C)[a]	R^2
3a	HCl	4.00	75.20	–89.57	40–60	0.995
		8.00	75.20	–71.69	40–60	0.995
	H_2SO_4	4.00	73.61	–93.84	40–60	0.997
		8.00	73.90	–71.69	40–60	0.996
	$HClO_4$	4.00	73.07	–101.63	40–60	0.991
		8.00	73.32	–99.51	40–60	0.997
3b	HCl	4.00	79.17	–102.1	40–60	0.998
3c	HCl	4.00	58.64	–95.92	30–50	0.994

[a] The measurements were made at 5 °C intervals.

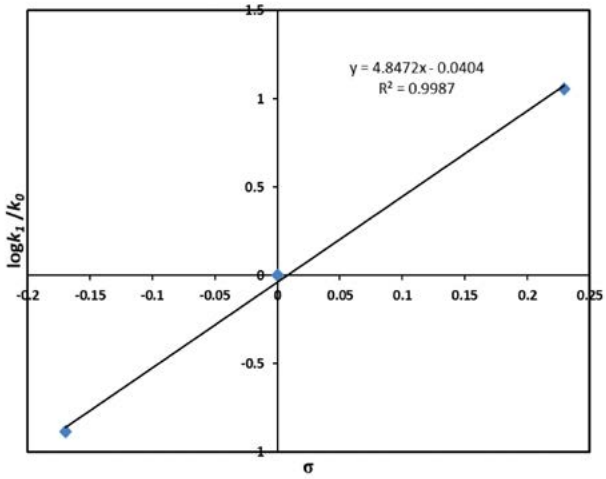

Figure 4. The plot of Hammett ρ versus log$k$ values for acid-catalysed hydrolysis (8.00 M HCl) of *N*-(4-substituedaryl) phthalimides at 50.0 ± 0.1 °C

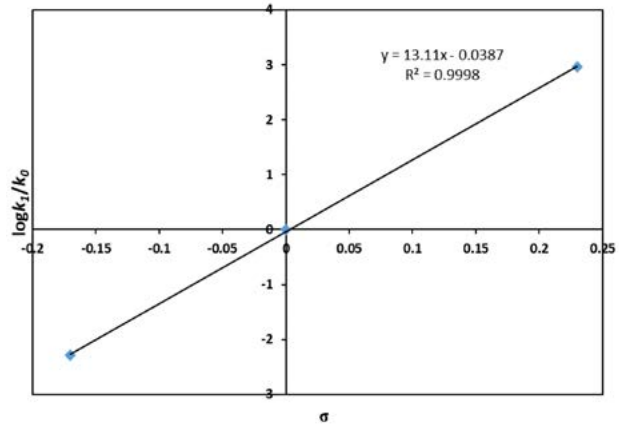

Figure 5. The plot of Hammett ρ versus log$k$ values for acid-catalyzed hydrolysis (4.00 M H_2SO_4) of *N*-(4-substituedaryl) phthalimides at 50.0 ± 0.1 °C

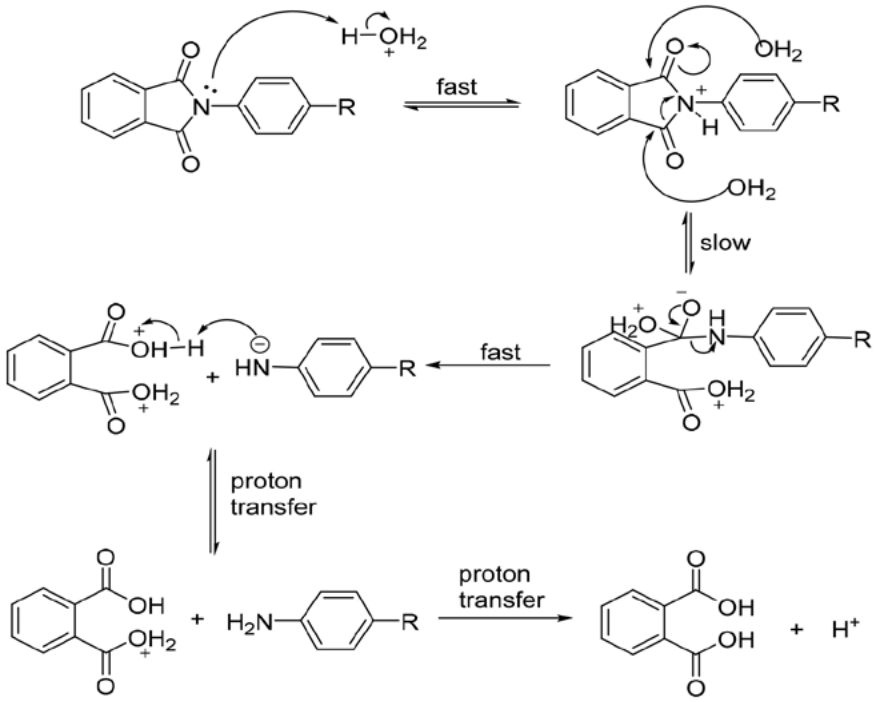

Scheme 3. A plausible acid-catalysed hydrolysis mechanism of the synthesized compounds

bonyl carbon atom as a nucleophile in the rate-determining step of the reaction. In intermediate step, aniline anion attack to protonated phthalic acid very fast. Then, the products of acid-catalyzed hydrolysis were observed to form phthalic acid and 4-chloroaniline.

3. 2. Antioxidant Evaluation

The DPPH˙ and ABTS˙⁺ scavenging activity results have shown in Table 4. Considering the molecules, compound **3c** is the most electronegative compound, then compound **3b** and then compound **3a** is electronegative. The N atom in the DPPH˙ and ABTS˙⁺ receives electrons from antioxidant compounds. The electronegativity of the N atom is higher than that of the Cl atom, the CH_3 molecule, and the H atom. Therefore, DPPH˙ scavenging activities are ranked from highest to lowest as **3c** >**3b** > **3a**, while ABTS˙⁺ radical scavenging activities are ordered as **3b**> **3c** >**3a** (Scheme 4). While there was a statistically significant difference between **3c**, α-tocopherol, BHA, **3b** and **3a** compounds in the DPPH˙ scavenging activity test, there was no significant difference between TBHQ and **3c** and α-tocopherol *($p < 0.05$)*. Whereas there was a statistically significant difference between **3c**, α-tocopherol, BHA, **3b,** and **3a** compounds in the ABTS˙⁺ scavenging activity test, there was no significant difference between BHA and TBHQ *($p < 0.05$)*. PerveenOrfali[51] reported that the DPPH˙ scavenging activity IC_{50} values of the *N*-(phenyl)phthalimide, *N*-(4-methylphenyl)phthalimide, and *N*-(4-chlorophenyl)phthalimide as 87.40 ± 0.15, 69.22 ± 0.12, and 91.70 ± 0.05 μM, respectively, and the BHA standard as 44.20 ± 0.06 μM. Nayab, Pulaganti, Chit-

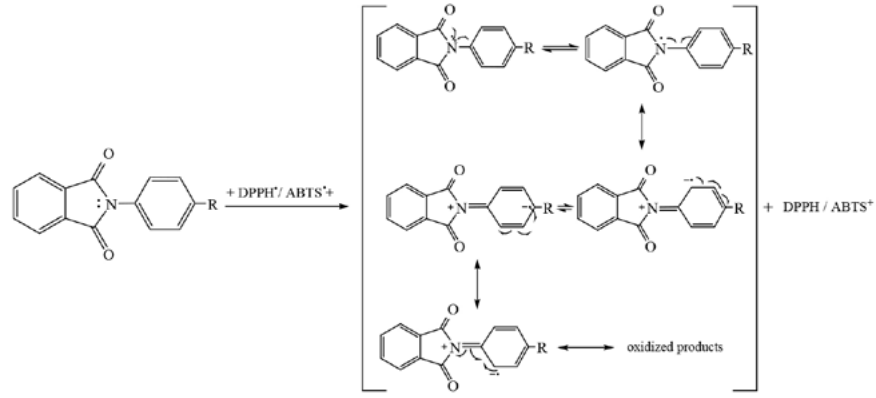

Scheme 4. The offer reactions of DPPH˙ and ABTS˙⁺ scavenging of the synthesized compounds

taOves[52] studied that the DPPH˙ scavenging activity (IC_{50}) of the *N*-(4-methylphenyl)phthalimide, and *N*-(4-chlorophenyl)phthalimide as 1.30 ± 0.05, and 1.40 ± 0.06 mg/mL, respectively, and the ascorbic acid standard as 0.10 ± 0.03 mg/mL. In our study, this assay observed *N*-(4-methylphenyl)phthalimide, and *N*-(4-chlorophenyl) phthalimide had lower activity.

Table 4. The results of antioxidant and enzyme inhibition activities of the synthesized compounds

Compounds and standards	Antioxidant Activity IC_{50} (µg/mL)		Enzyme Inhibition Activity IC_{50} (µg/mL)		
	DPPH˙	ABTS˙⁺	AChE	BChE	Urease
3a	95.7 ± 0.8^{e}	79.9 ± 1.4^{d}	13.1 ± 0.2^{b}	6.8 ± 0.1^{a}	17.7 ± 0.6^{b}
3b	20.1 ± 0.0^{d}	6.4 ± 1.6^{ab}	9.6 ± 0.5^{a}	7.4 ± 0.4^{a}	17.3 ± 0.0^{b}
3c	2.0 ± 0.1^{a}	56.8 ± 1.5^{c}	29.6 ± 0.2^{c}	13.6 ± 0.6^{b}	10.5 ± 0.0^{a}
BHA	5.7 ± 0.5^{c}	3.8 ± 0.0^{a}	NU	NU	NU
TBHQ	3.2 ± 0.3^{ab}	4.0 ± 0.0^{a}	NU	NU	NU
α-tocopherol	3.9 ± 0.1^{b}	9.4 ± 0.2^{b}	NU	NU	NU
Galantamine	NU	NU	14.4 ± 0.0^{b}	49.4 ± 0.0^{c}	NU
Thiourea	NU	NU	NU	NU	26.2 ± 0.0^{c}
F-value	17512.1	1977.9	1604.3	5876.0	854.2

NU: Not use, The letters a, b, c, and d are statistically significant indicators. a; refers to statistical significance corresponding to high activity. b and c; represent statistical significance corresponding to moderate activity. d; refers to statistical significance corresponding to low activity. e; refers to statistical significance corresponding to very low activity. In all tests $p < 0.05$. F-values are based on one way ANOVA for individual instars

3. 3. Enzyme Inhibition Activity

The results of urease, AChE, and BChE inhibition activity have shown in Table 4. When comparing the activities of the samples with the standards and among themselves, it was observed that the compound **3c** had the best urease inhibition activity. It is possible that the reason **3c** sample was most effective against urease is that it has the chloride (negative ion) which in turn contributed to its stability at the active site of urease, that contain positively charged nickel atomes. In contrast, compounds **3a** and **3b** had higher activity than the standard as well. Ranking the compounds from high activity to low activity; are shaped like **3c, 3b, 3a,** and thiourea. While there was a statistically significant difference between **3c**, **3b** and thiourea compounds in urease inhibition activity test, there was no significant difference between **3a** and **3b** *($p < 0.05$)*. Besides, it was determined that the compound **3b** sample had the best AChE inhibition activity, whereas compound **3c** had the lowest activity. The compounds from high activity to low activity; are shaped like **3b, 3a**, galantamine, and **3c**. While there was a statistically significant difference between **3c**, **3b**, **3a,** and galantamine compounds in AChE inhibition activity test, there was no significant difference between **3a** and galantamine *($p < 0.05$)*. Also, the compound **3a** sample had the best BChE inhibition activity, while compounds **3b** and **3c** had the higher activity than the standard as well . The compounds from high to low activity; are shaped like **3a, 3b, 3c,** and galantamine. While there was a statistically significant difference between **3c**, **3a,** and galantamine compounds in BChE inhibition activity test, there was no significant difference between **3a** and **3b** *($p < 0.05$)*.

3. 4. Molecular Docking Analysis

The created docked complexes were analyzed based on the minimum affinity energy value (kcal/mol) and binding interaction patterns; the most stable poses with the lowest affinity energy value were taken for further analysis. So, we mainly focused our work on the ligands (synthetic compounds) interactions within these stable poses, which could inhibit the enzyme activity (Table 5). Docking results improved that **3b** showed the best binding among molecules at (−9.7 kcal/mol) affinity energy value within acetylcholinesterase, which was the best among samples. As for the remaining enzyme, **3b** and **3c** predict the same binding affinity energy value at (−9.0 kcal/mol) to butyrylcholinesterase. However, compound **3b** showed the minimum energy value (−8.6 kcal/mol). At the same time, **3a** gave (−7.8 kcal/mol) energy value which was somewhat lower than other compounds against urease. These poses with the lowest value (highest binding score) had been selected to analyze their interaction with enzyme residues.

As seen in Figure 6, the compounds (**3a-c**) have a significant interaction pose placed in the hollow at the AChE surface predicted interaction via hydrogen bonds and hydrophobic interactions with the amino acids surrounding it, as shown in the close-up part of the exact figure. Further, synthetic compounds demonstrate their ability to form potential hydrogen bonds within BChE at

histidine 438. Serine 198 amino acids also showed the possibility of attractive electrostatic interactions with the near amino acids Figure 7. Furthermore, as shown in Figure 8, **3a**, **3b,** and **3c** had bound to the urease enzyme via the same site. This linkage, as can be seen in the zoom-in part of Figure 8, it was done by a hydrogen bond between the compounds' oxygen atom and the same atom from the tyrosine 32 from the enzyme for both **3b** and **3c** and with the second bond between the other oxygen of **3a** and lysine 716 amino acid.

We have also exported 2D interaction diagrams of ligands (using the Ligplot+) with the highest binding

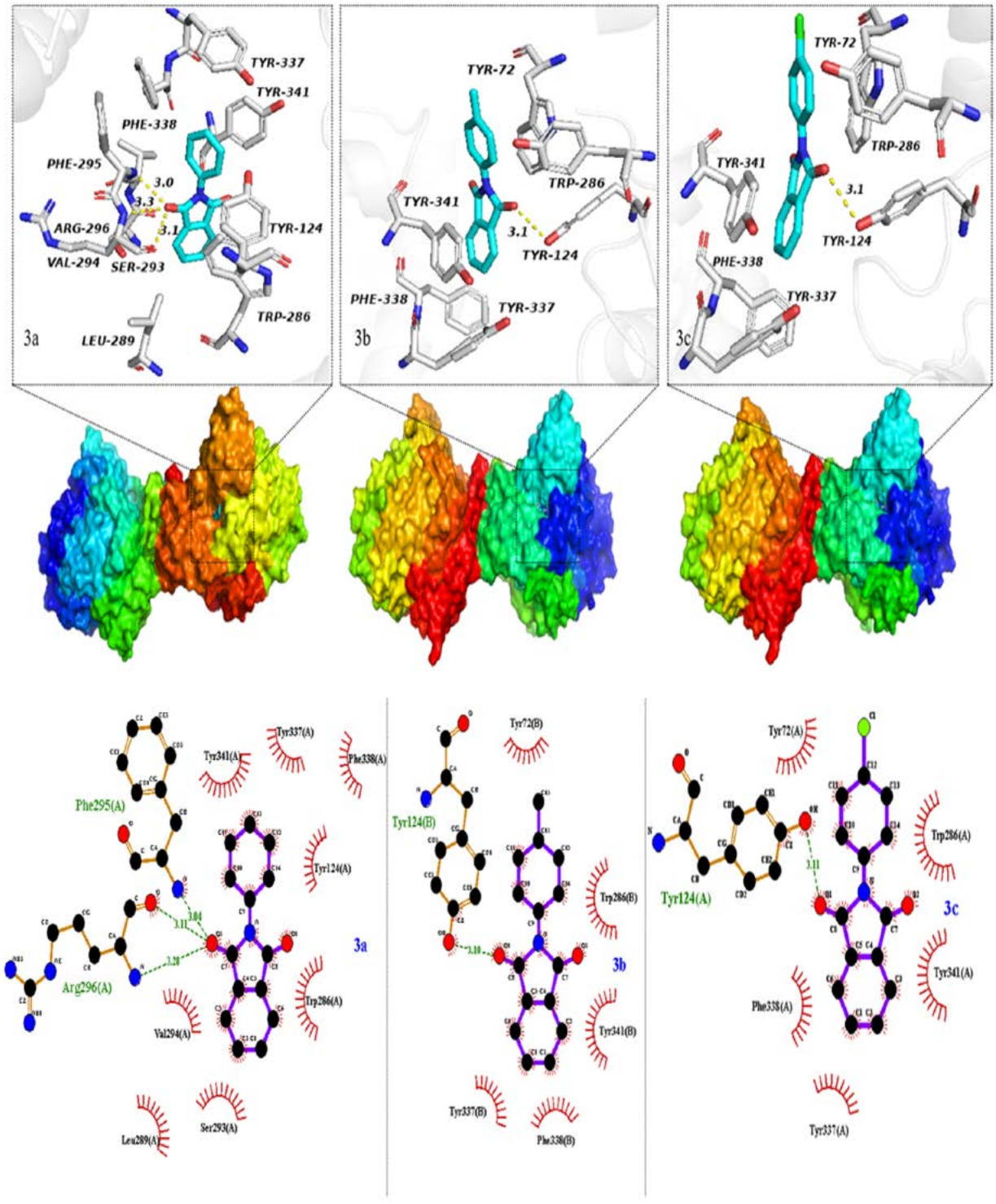

Figure 6. 3D and 2D detailed binding modes of the best pose of synthesized compounds into active catalytic site of AChE

scores and demonstrated that all compounds had succeeded in forming hydrogen bonds and hydrophobic interactions into the active sites of enzymes (Figures 6-8). These results were identical to what was obtained by the PyMOL program analyzing results and the 3D diagrams; the closed state of compound-AChE complexes in Figure 6 exposed that **3a** compound, in addition to creating hydrogen bonds with two amino acids (Phe295 and Arg396), it can also develop kinds of hydrophobic interactions with (Val294, Leu289, Ser293, Trp286, Tyr124, Phe338, Tyr337, and Tyr341). However, **3b** and **3c** could be linked to AChE by a hydrogen bond at (Tyr124) and form a nonpolar attrac-

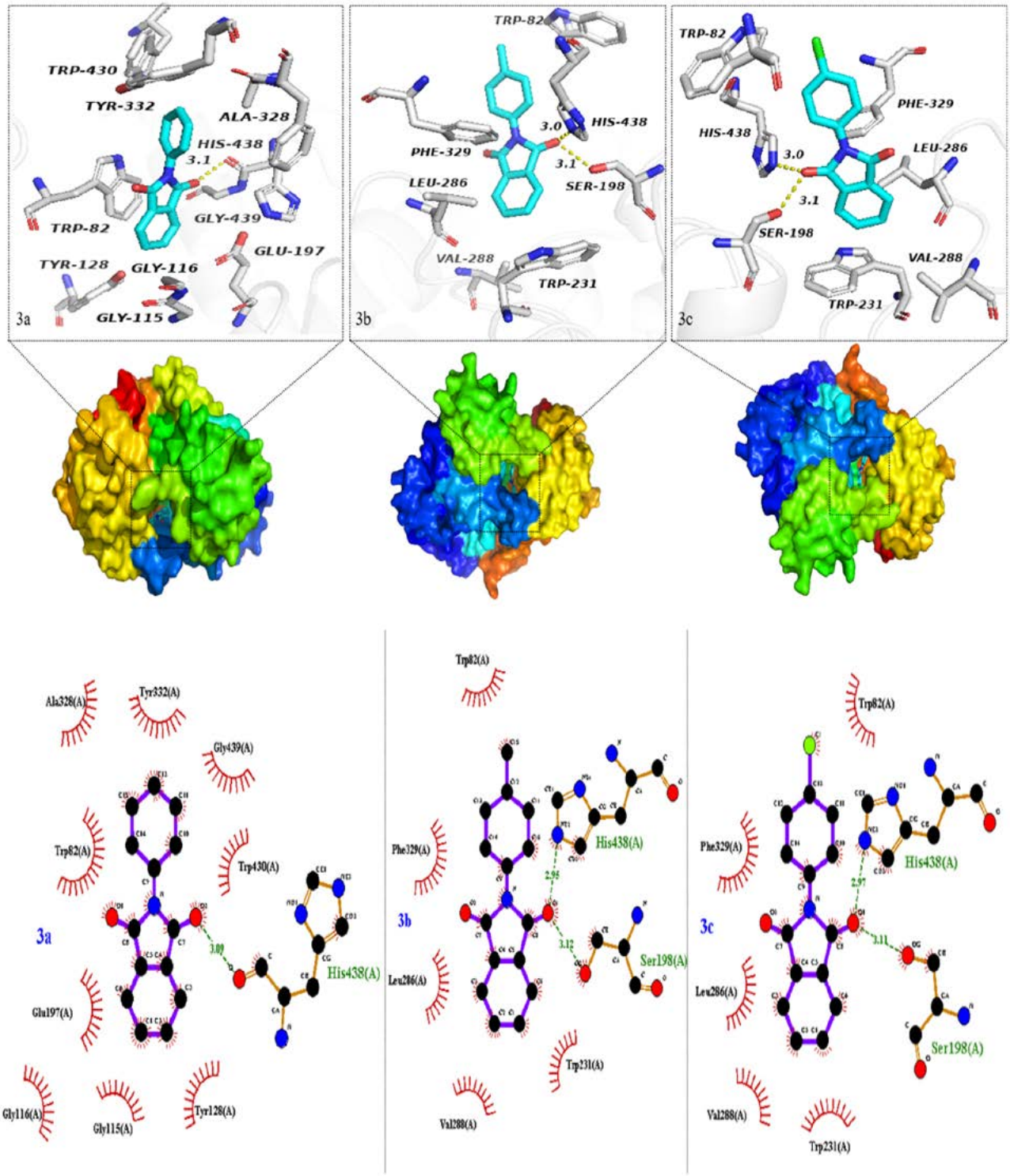

Figure 7. 3D and 2D detailed binding modes of the best pose of synthesized compounds into the active catalytic site of BChE

tion with (Tyr72, Trp286, Tyr341, Phe338, and Tyr337). For the BChE, as shown in Figure 7, **3a** compound is predicted to create a hydrogen bond with the His438 amino acid and been attracted by interaction with (Trp430, Gly439, Tyr332, Ala328, Trp82, Glu179, Gly116, Gly115 and Tyr128). At the same time, **3b** and **3c** compounds could form a hydrogen bond with (His438 and Ser198) and be hydrophobically affected by (Trp82, Phe329, Leu286, Val288, and Trp231) amino acids. As for the urease enzyme, **3a** is predicted to form an H-bond with (Tyr32 and Lys716) and form hydrophobic interaction with (Val744, Thr33, Val36, Glu742, Phe712, Asp730, and Glu718), whereas **3b** and **3c** are more likely to be bonded to (Tyr32) via H-bond and attracted by hydrophobic interaction to (Val744, Thr33, Val36, Ala37, Glu742, Phe712, Asp730, Lys716, and Glu718) simultaneously (Figure 8).

Table 5. Binding scores for synthesized compounds with target enzymes

Compounds	Affinity (kcal/mol)		
	AChE	BChE	Urease
3a	–8.3	–8.7	–7.8
3b	–9.7	–9.0	–8.6
3c	–9.5	–9.0	–8.5

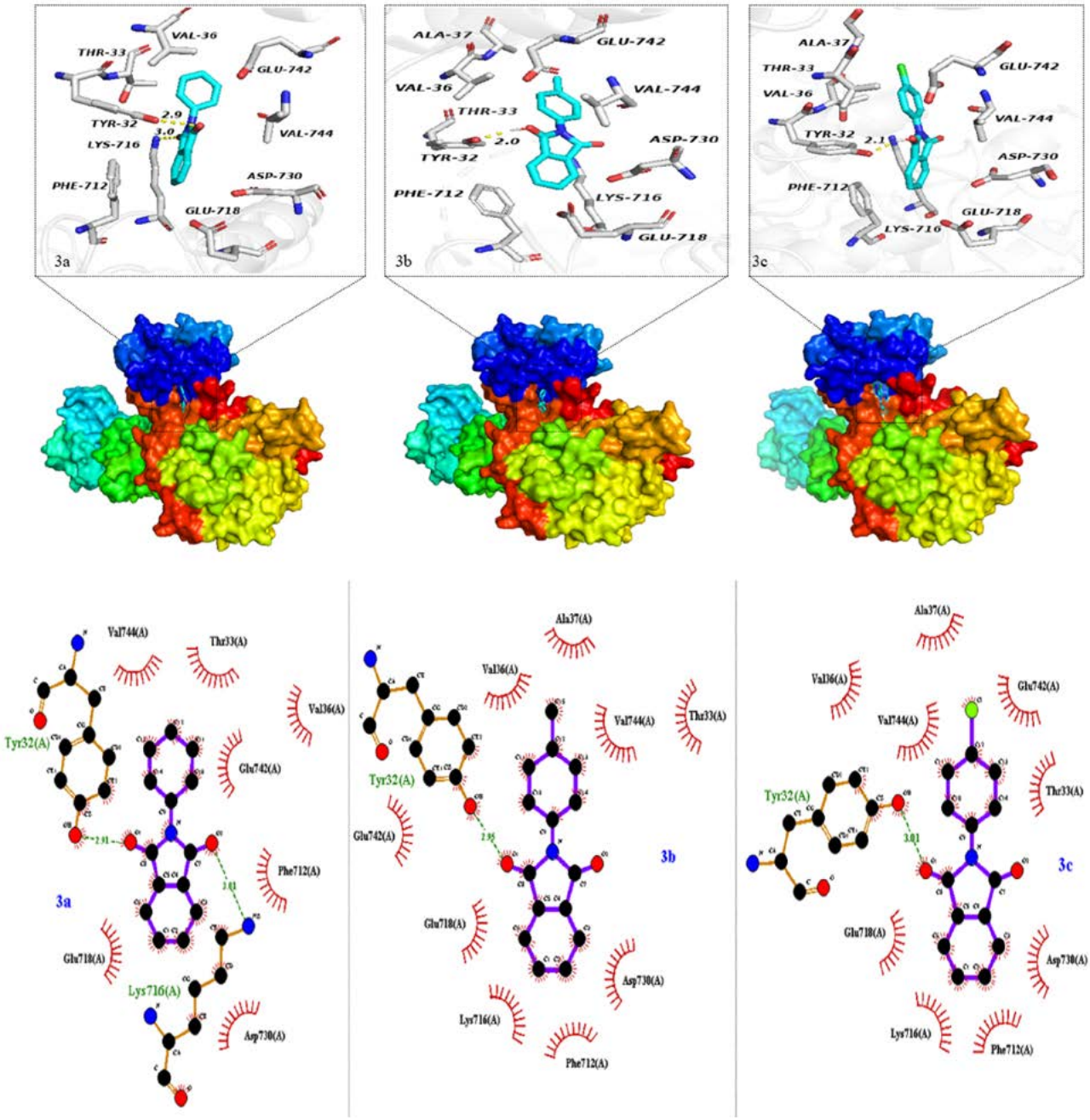

Figure 8. 3D and 2D detailed binding mode of the best-pose of synthesized compounds into the active catalytic site of urease

4. Conclusions

The acid-catalysed hydrolysis mechanism of *N*-(4-substituedphenyl) phthalimides **3a–c** was examined. Analyses of the data by the Excess Acidity treatment, entropy of activation, and substituent effect are consistent with an A-2 mechanism in the whole range of acidity. Catalytic order of strong acids for the acid catalyzed hydrolysis of the compounds studied were as $HCl \cong H_2SO_4 > HClO_4$ in all acidity ranges. These are the characteristics of an A–2 mechanism. Furthermore, two moles of water were involved as a nucleophile in the reaction rate-determining step of the A–2 mechanism.

When the antioxidant activities of the phthalimides; it was observed that the compound **3c** sample had the best $DPPH^{\cdot}$ scavenging activity. Ranking the compounds from high to low activity; are shaped like **3c,** TBHQ, α-tocopherol, BHA, **3b**, **3a**. Besides, it was determined the compound **3b** sample had the best $ABTS^{\cdot+}$ radical scavenging activity. Ranking the compounds from high activity to low activity; are shaped like BHA, TBHQ, **3b**, α-tocopherol, **3c**, **3a**. As for the enzyme inhibition activities of the phthalimides; it was observed that the compound **3c** sample had the best urease inhibition activity. In contrast, compounds **3b** and **3a** were determined higher activities from thiourea. Thus, these compounds can be used as urease inhibitors. It was determined that compound **3b** sample had the best AChE inhibition activity, whereas compound **3a** was determined to have higher activities from galantamine. Thereby, compounds **3b** and **3a** can be used as acetylcholinesterase inhibitors. Also, it was observed the compound **3a** sample had the best BChE inhibition activity, while the compounds **3b** and **3c** were determined to have higher activities from galantamine. So, compounds **3b** and **3c** can be used as butyrylcholinesterase inhibitors.

All synthesized compounds successfully docked to urease, acetylcholinesterase, and butyrylcholinesterase binding sites. Among these molecules, **3b** has the best binding score (–9.7 kcal/mol) with acetylcholinesterase; further, simulation results were harmonious with *in-vitro* inhibition activity results for the same enzymes.

Declarations

Ethics approval

No permissions are required for this work.

Competing interests

The authors declare that they have no conflict of interest.

Funding

We would like to thank Ondokuz Mayis University (Grant No. PYO.FEN.1904.12.027) for its financial support of this work.

Availability of data and materials

If data is requested, the relevant author will share it with you or reviewer.

Author Contributions

Hasan Yakan: Synthesis, Characterization, Kinetic Studies, Writing–Review. **Seyhan Ozturk**: Synthesis, Characterization, Writing–Review, Visualization & Editing. **Elvan Uyar Tolgay**: Synthesis, Characterization, Kinetic Studies. **Semiha Yenigun**: Antioxidant Activity and Enzyme Inhibitor Studies, Writing–Review. **Sarmad Marah**: Molecular Docking Studies, Writing–Review. **Tugrul Doruk**: Molecular Docking Studies, Writing–Review. **Tevfik Ozen**: Biologic Studies, Writing–Review, Supervision. **Halil Kutuk**: Kinetic Studies, Writing–Review, Supervision.

Acknowledgments

The synthesis, structure elucidation, and kinetic-acidic hydrolysis assay parts of this study belong to Elvan Uyar Tolgay master thesis at Ondokuz Mayis University. The authors thank Dr. Mohammad Maher Jerry for checking and proofreading the article.

Supplementary Material

Kinetic data of the compounds are given in the supporting information.

5. References

1. A. Khalil, M. Berghot, M. Gouda, *European journal of medicinal chemistry* **2010**, *45*, 1552–1559. **DOI:**10.1016/j.ejmech.2009.12.064
2. L. d. M. Lima, P. Castro, A. L. Machado, C. A. M. Fraga, C. Lugnier, V. L. G. de Moraes, E. J. Barreiro, *Bioorganic & medicinal chemistry* **2002**, *10*, 3067–3073. **DOI:**10.1016/S0968-0896(02)00152-9
3. S. H. L. Kok, R. Gambari, C. H. Chui, M. C. W. Yuen, E. Lin, R. S. M. Wong, F. Y. Lau, G. Y. M. Cheng, W. S. Lam, S. H. Chan, *Bioorganic & medicinal chemistry* **2008**, *16*, 3626–3631. **DOI:**10.1016/j.bmc.2008.02.005
4. F. A. Santos, M. L. Almeida, V. A. Silva, D. C. Viana, M. C. Pereira, A. S. Lucena, M. G. Pitta, M. R. Galdino-Pitta, M. J. de Melo Rêgo, I. da Rocha Pitta, *Med. Chem. Res.* **2022**, *31*, 108–119. **DOI:**10.1007/s00044-021-02821-7
5. J. L. Santos, P. R. Yamasaki, C. M. Chin, C. H. Takashi, F. R. Pavan, C. Q. Leite, *Bioorganic & medicinal chemistry* **2009**, *17*, 3795–3799. **DOI:**10.1016/j.bmc.2009.04.042
6. J. Singh, T. Singha, A. Naskar, M. Kundu, R. K. Harwansh, A. Mondal, T. Ghosh, T. Maity, *Pharmacologyonline* **2011**, *2*, 976–987.
7. S. C. Annedi, J. Ramnauth, S. P. Maddaford, P. Renton, S. Ra-

khit, G. Mladenova, P. Dove, S. Silverman, J. S. Andrews, M. D. Felice, *Journal of medicinal chemistry* **2012**, *55*, 943–955. **DOI:**10.1021/jm201564u
8. P. Appelbaum, P. Hunter, *International journal of antimicrobial agents* **2000**, *16*, 5–15. **DOI:**10.1016/S0924-8579(00)00192-8
9. a) A. Aliabadi, A. Foroumadi, A. Mohammadi-Farani, M. G. Mahvar, *Iranian journal of basic medical sciences* **2013**, *16*, 1049;
b) C.-L. Chi, L. Xu, J.-J. Li, Y. Liu, B.-Q. Chen, *Med. Chem. Res.* **2022**, *31*, 120–131. **DOI:**10.1007/s00044-021-02823-5
10. Z. Sang, K. Wang, H. Wang, L. Yu, H. Wang, Q. Ma, M. Ye, X. Han, W. Liu, *Bioorganic & medicinal chemistry letters* **2017**, *27*, 5053–5059. **DOI:**10.1016/j.bmcl.2017.09.055
11. X. Collin, J.-M. Robert, G. Wielgosz, G. Le Baut, C. Bobin-Dubigeon, N. Grimaud, J.-Y. Petit, *Eur. J. Med. Chem.* **2001**, *36*, 639–649. **DOI:**10.1016/S0223-5234(01)01254-5
12. W. D. Figg, S. Raje, K. S. Bauer, A. Tompkins, D. Venzon, R. Bergan, A. Chen, M. Hamilton, J. Pluda, E. Reed, *J. Pharm. Sci.* **1999**, *88*, 121–125. **DOI:**10.1021/js980172i
13. E. Atra, E. I. Sato, *Clin. Exp. Rheumatol.* **1993**, *11*, 487–493.
14. a) H. R. Lobo, B. S. Singh, G. S. Shankarling, *Green Chemistry Letters and Reviews* **2012**, *5*, 487–533;
DOI:10.1080/17518253.2012.669500
b) M. Sani, G. Fossati, F. Huguenot, M. Zanda, *Angew. Chem.* **2007**, *119*, 3596–3599. **DOI:**10.1002/ange.200604557
15. a) L. Wang, Z. Kuang, D. Zhang, Y. Gao, M. Ying, T. Wang, *Biomed. Pharmacother.* **2021**, *133*, 110978;
DOI:10.1016/j.biopha.2020.110978
b) Z. Zhou, X. Yuan, D. Long, M. Liu, K. Li, Y. Xie, *Spectrochimica Acta Part A: Molecular and Biomolecular Spectroscopy* **2021**, *246*, 118927. **DOI:**10.1016/j.saa.2020.118927
16. a) N. Kaushik, N. Kumar, A. Kumar, *Int. J. Pharm. Pharm. Sci.* **2015**, *7*, 120–123; b) S. Oyedemi, G. Bradley, A. Afolayan, *African Journal of pharmacy and pharmacology* **2010**, *4*, 070-078.
17. C. Zhang, D. Chen, X. Liu, *Molecular & Cellular Toxicology* **2016**, *12*, 45–52. **DOI:**10.1007/s13273-016-0007-0
18. M. Mrdaković, L. Ilijin, M. Vlahović, D. Matić, A. Gavrilović, A. Mrkonja, V. Perić-Mataruga, *Chemosphere* **2016**, *159*, 565-569. **DOI:**10.1016/j.chemosphere.2016.06.059
19. P. Taslimi, C. Caglayan, V. Farzaliyev, O. Nabiyev, A. Sujayev, F. Turkan, R. Kaya, İ. Gulçin, *Journal of biochemical and molecular toxicology* **2018**, *32*, e22042.
DOI:10.1002/jbt.22042
20. G. Zengin, I. Senkardes, A. Mollica, C. M. N. Picot-Allain, G. Bulut, A. Dogan, M. F. Mahomoodally, *Computational biology and chemistry* **2018**, *75*, 111–119.
DOI:10.1016/j.compbiolchem.2018.05.005
21. Z. Amtul, R. Siddiqui, M. Choudhary, *Current medicinal chemistry* **2002**, *9*, 1323–1348.
DOI:10.2174/0929867023369853
22. M. Amin, M. S. Iqbal, R. W. Hughes, S. A. Khan, P. A. Reynolds, V. I. Enne, Sajjad-ur-Rahman, A. S. Mirza, *Journal of Enzyme Inhibition and Medicinal Chemistry* **2010**, *25*, 383–390.
DOI:10.3109/14756360903179518
23. a) S. Kumar, S. M. Lim, K. Ramasamy, M. Vasudevan, S. A. A. Shah, M. Selvaraj, B. Narasimhan, *Chemistry Central Journal* **2017**, *11*, 1–16; **DOI:**10.1186/s13065-017-0322-0
b) S. Zhang, B. Qiu, J. Zhu, M. Khan, X. Liu, *Spectrochimica Acta Part A: Molecular and Biomolecular Spectroscopy* **2018**, *203*, 13–18. **DOI:**10.1016/j.saa.2018.05.077
24. a) M. Hanif, K. Shoaib, M. Saleem, N. Hasan Rama, S. Zaib, J. Iqbal, *International Scholarly Research Notices* **2012**, *2012*;
DOI:10.5402/2012/928901
b) N. Yayli, G. Kılıç, G. Celik, N. Kahriman, Ş. Kanbolat, A. Bozdeveci, Ş. A. Karaoğlu, R. Aliyazıcıoğlu, H. E. Sellitepe, İ. S. Doğan, *Turk. J. Chem.* **2021**, *45*, 788–804;
DOI:10.3906/kim-2012-25
c) A. M. S. Mascarenhas, R. B. M. de Almeida, M. F. de Araujo Neto, G. O. Mendes, J. N. da Cruz, C. B. R. Dos Santos, M. B. Botura, F. H. A. Leite, *Journal of Biomolecular Structure and Dynamics* **2021**, *39*, 6021–6030;
DOI:10.1080/07391102.2020.1796791
d) N. Yaylı, G. Kılıç, N. Kahriman, Ş. Kanbolat, A. Bozdeveci, Ş. A. Karaoğlu, R. Aliyazıcıoğlu, H. E. Sellitepe, İ. S. Doğan, A. Aydın, *Bioorg. Chem.* **2021**, *115*, 105183;
DOI:10.1016/j.bioorg.2021.105183
e) H. Yakan, Ü. M. Koçyiğit, H. Muğlu, M. Ergul, S. Erkan, E. Güzel, P. Taslimi, İ. Gülçin, *Journal of Biochemical and Molecular Toxicology* **2022**, *36*, e23018; **DOI:**10.1002/jbt.23018
f) Ü. M. Koçyiğit, P. Taslimi, B. Tüzün, H. Yakan, H. Muğlu, E. Güzel, *Journal of Biomolecular Structure and Dynamics* **2022**, *40*, 1–11;
g) Y. V. Martynenko, O. M. Antypenko, O. A. Brazhko, I. B. Labenska, S. I. Kovalenko, *Acta Chimica Slovenica* **2019**, *66*, 145–154. **DOI:**10.17344/acsi.2018.4731
25. a) B. Garcia, F. Hoyuelos, S. Ibeas, J. Leal, *The Journal of organic chemistry* **2006**, *71*, 3718–3726; **DOI:**10.1021/jo052561k
b) T. H. Lowry, K. S. Richardson, *Mechanism and theory in organic chemistry*, Harper & Row New York, **1987**, p.
26. a) C. Bunton, J. Fendler, *The Journal of Organic Chemistry* **1966**, *31*, 3764–3771; **DOI:**10.1021/jo01349a064
b) D. Jacewicz, J. Pranczk, A. Dąbrowska, L. Chmurzyński, *Reaction Kinetics, Mechanisms and Catalysis* **2010**, *100*, 11–20.
27. K. Yates, R. A. McClelland, *Journal of the American Chemical Society* **1967**, *89*, 2686–2692.
DOI:10.1021/ja00987a033
28. K. K. Ghosh, S. Ghosh, *The Journal of Organic Chemistry* **1994**, *59*, 1369–1374. **DOI:**10.1021/jo00085a028
29. L. L. Schaleger, F. Long, *Adv. Phys. Org. Chem.* **1963**, *1*, 1-33.
DOI:10.1016/S0065-3160(08)60276-2
30. R. A. Y. Jones, *Physical and mechanistic organic chemistry*, Cambridge University Press, Cambridge, **1979**, p.
31. a) R. A. Cox in *Excess acidities*, *Vol. 35* Elsevier, **2000**, pp. 1-66; **DOI:**10.1016/S0065-3160(00)35011-0
b) R. A. Cox, K. Yates, *Journal of the American Chemical Society* **1978**, *100*, 3861–3867; **DOI:**10.1021/ja00480a033
c) R. A. Cox, K. Yates, *Can. J. Chem.* **1979**, *57*, 2944–2951.
DOI:10.1139/v79-479
32. H. Kutuk, Y. Bekdemir, N. Turkoz, *Phosphorus, Sulfur, and Silicon and the Related Elements* **2006**, *181*, 931–937.

DOI:10.1080/10426500500272186
33. H. Kutuk, S. Ozturk, *Phosphorus, Sulfur, and Silicon* **2009**, *184*, 332–340. **DOI:**10.1080/10426500802119655
34. H. Kutuk, J. Tillett, *Phosphorus, Sulfur, and Silicon and the Related Elements* **1993**, *85*, 217–224. **DOI:**10.1080/10426509308038201
35. H. Kutuk, H. Yakan, *Phosphorus, Sulfur, and Silicon and the Related Elements* **2011**, *186*, 1460–1469. **DOI:**10.1080/10426507.2010.517584
36. M. M. Langade, *Der Pharm Chem* **2011**, *3*, 283–286.
37. H. Asefi, J. G. Tillett, *Journal of the Chemical Society, Perkin Transactions 2* **1979**, 1579–1582. **DOI:**10.1039/p29790001579
38. B. Bujnicki, J. Drabowicz, M. Mikołajczyk, A. Kolbe, L. Stefaniak, *The Journal of organic chemistry* **1996**, *61*, 7593–7596. **DOI:**10.1021/jo960205j
39. Y. Bekdemir, A. Gediz Erturk, H. Kutuk, *J. Phys. Org. Chem.* **2014**, *27*, 94–98. **DOI:**10.1002/poc.3242
40. Z. Mei-Yun, L. Yi-Qun, X.-m. Xu, *Synth. Commun.* **2003**, *33*, 3777–3780. **DOI:**10.1081/SCC-120025187
41. a) M. S. Blois, *Nature* **1958**, *181*, 1199–1200; **DOI:**10.1038/1811199a0
b) H. Muğlu, H. Yakan, A. G. A. Misbah, M. S. Çavuş, T. K. Bakır, *Res. Chem. Intermed.* **2021**, *47*, 4985–5005; **DOI:**10.1007/s11164-021-04576-7
c) H. Muğlu, M. Akın, M. S. Çavuş, H. Yakan, N. Şaki, E. Güzel, *Computational Biology and Chemistry* **2022**, *96*, 107618; **DOI:**10.1016/j.compbiolchem.2021.107618
d) H. Yakan, *Res. Chem. Intermed.* **2020**, *46*, 3979–3995; **DOI:**10.1007/s11164-020-04185-w
e) H. Yakan, M. S. Çavuş, B. Z. Kurt, H. Muğlu, F. Sönmez, E. Güzel, *J. Mol. Struct.* **2021**, *1239*, 130495; **DOI:**10.1016/j.molstruc.2021.130495
f) H. Yakan, T. K. Bakır, M. S. Çavuş, H. Muğlu, *Res. Chem. Intermed.* **2020**, *46*, 5417–5440. **DOI:**10.1007/s11164-020-04270-0
42. a) R. Re, N. Pellegrini, A. Proteggente, A. Pannala, M. Yang, C. Rice-Evans, *Free radical biology and medicine* **1999**, *26*, 1231–1237; **DOI:**10.1016/S0891-5849(98)00315-3
b) B. Dechayont, P. Ruamdee, S. Poonnaimuang, K. Mokmued, J. Chunthorng-Orn, *Journal of Botany* **2017**, *2017*. **DOI:**10.1155/2017/8310275
43. L. Zhang, S. B. Mulrooney, A. F. Leung, Y. Zeng, B. B. Ko, R. P. Hausinger, H. Sun, *Biometals* **2006**, *19*, 503–511. **DOI:**10.1007/s10534-005-5449-0
44. a) G. L. Ellman, K. D. Courtney, V. Andres Jr, R. M. Featherstone, *Biochemical pharmacology* **1961**, *7*, 88–95; **DOI:**10.1016/0006-2952(61)90145-9
b) A. B. Özçelik, M. Gökçe, I. Orhan, M. F. Sahin, *FABAD Journal of Pharmaceutical Sciences* **2010**, *35*, 153.
45. H. M. Berman, J. Westbrook, Z. Feng, G. Gilliland, T. N. Bhat, H. Weissig, I. N. Shindyalov, P. E. Bourne, *Nucleic acids research* **2000**, *28*, 235–242.
46. O. Trott, A. J. Olson, *Journal of computational chemistry* **2010**, *31*, 455–461.
47. R. A. Laskowski, J. Jabłońska, L. Pravda, R. S. Vařeková, J. M. Thornton, *Protein science* **2018**, *27*, 129–134. **DOI:**10.1002/pro.3289
48. C. A. Bunton, J. H. Crabtree, L. Robinson, *Journal of the American Chemical Society* **1968**, *90*, 1258–1265. **DOI:**10.1021/ja01007a027
49. J. Liang, J. Lv, J.-c. Fan, Z.-c. Shang, *Synthetic Communications®* **2009**, *39*, 2822–2828. **DOI:**10.1080/00397910802474966
50. A. Bagno, G. Scorrano, R. M. O'Ferrall, *Reviews of chemical intermediates* **1987**, *7*, 313–352. **DOI:**10.1007/BF03155656
51. S. Perveen, R. Orfali, *Journal of Chemistry* **2018**, *2018*. **DOI:**10.1155/2018/5198325
52. P. S. Nayab, M. Pulaganti, S. K. Chitta, M. Oves, *Bangladesh Journal of Pharmacology* **2015**, *10*, 703–713. **DOI:**10.3329/bjp.v10i3.23637

Povzetek

Kislinsko katalizirano hidrolizo N-(p-substituiranih fenil) ftalimidov v treh različnih kislinah smo proučili pri 50,0 ± 0,1 °C. Uporabljena sta bila dva različna testa antioksidativne aktivnosti, in sicer določitev DPPH• in odstranjevanje DPPH•, ter trije različni testi inhibitorne aktivnosti encimov, in sicer inhibicija ureaze, acetilholinesteraze (AChE) in butilholinesteraze (BChE). Spojina 3c (2,03 μg/ml) je imela večjo antioksidativno aktivnost kot druge spojine in standardi glede na test DPPH. Pri testu AChE sta imeli spojini 3a in 3b (13,13 in 9,59 μg/ml) večjo inhibitorno aktivnost encima kot standard galantamin (14,37 μg/ml). Pri testih BChE in ureaze so imele vse spojine (6,84-13,60 in 10,49-17,73 μg/ml) večjo inhibitorno aktivnost encimov kot standard galantamin (49,40 μg/ml) oz. tiourea (26,19 μg/ml). S simulacijami molekularnega sidranja smo preučili interakcijo vsake od treh spojin z aktivnimi mesti encimov AChE, BChE in ureaze.